J. Nig. Ass. Math. Phys.
Vol. 4 (2000)

ELECTRIC NUSSELT NUMBER IN A CLOSED CYLINDRICAL CONTAINER FILLED WITH TWO IMMISCIBLE FLUIDS

M. F. HAQUE; O.W. OLASOJI AND E.D. MSHELIA
PHYSICS DEPARTMENT,
ABUBAKAR TAFAWA BALEWA UNIVERSITY, P.M.B. 0248
BAUCHI, NIGERIA.

ABSTRACT

Electric Nusselt number (ENN) in a closed cylindrical container filled with two immiscible fluids Δ/water, Δ/ethyl alcohol, Δ/silicon oil and Δ/kerosene (where Δ stands for air, 0_2, N_2 and F_{12}) is measured under the influence of electric fields. The measurement is carried out using a single platinum wire (diameter = 0.025 mm) mounted along the axis of the cylindrical container, made of copper (diameter = 53.0 mm). ENN is measured with gas/liquid ratios of one-to-three, one-to-one and three-to-one respectively. The ENN data have been correlated by dimensional analysis. The data have been compared with the predicted relations and analytical expression and is well correlated over the range of the Rayleigh number from 2.0×10^4 to 4.0×10^7. A_n empirical correlation relationship is proposed to evaluate the efficiency of convection and the results for gas/liquid combinations in the combination ratios one-to-three and three-to-one are presented.

1. INTRODUCTION

Electrical Nusselt Number (ENN) in a cylindrical container filled with two immiscible fluids (a gas and a liquid) is of great importance for many natural and industrial processes. Among other technical applications, the crystal growth process of metals, semiconductor silicon, ceramics and polymers involve molten and vapor phases and is controlled by heat and mass transfer process. The past few years have witnessed an explosive growth of efforts in the preparation and processing of crystal growth in space, but the fluid mechanics of such technical processes, the origins and consequences of convective transport, under the influence of electric fields are not adequately understood.

The objective of the present study is to gain some insight into the heat transfer phenomena under the influence of a non-uniform electric field. The system under consideration consists of a cylindrical container with a heated wire mounted along the axis of the cylinder. Due to the fact that the geometric shape of the system under consideration is connected with numerous technical applications, a number of studies have investigated the heat transfer phenomena of gases, liquids and gas/liquid combination in horizontal cylindrical container, and also containers of concentric and eccentric cylindrical annular shape. Senftleben [1-3] studied electroconvection in gases in a cylindrical container, with a heated wire passing through the axis of the cylinder and also those of Ahasman and Kronig [4] in 1950 on liquids. Heat transfer of air/water layer

in a horizontal cooled circular tube was investigated by Fukusako and Takahashi [5]. Oosthuizen and Paul [6] studied natural convective heat transfer in a closed square container filled with a liquid and a gas. Natural convective heat transfer in horizontal enclosures of concentric and eccentric cylindrical annular shape was also studied by Kuehn and Goldstein [7] for early works and by Projahn and Beer [8] for recently published works, but the investigation concerning the multiple fluid system under the influence of electric fields are scarce.

Much research work has been performed by the author and his co-workers concerning the electroconvective heat transfer in a horizontal and vertical cylinder filled with a gas or a liquid, see for example Refs. [9-12]. There are however, certain situations where the convection in gas/liquid fluid system would be desired. The present work has been undertaken to study the electroconvection in gas/liquid fluid combination such as Δ/water, Δ/ethyl alcohol, Δ/silicon oil and Δ/kerosene (Δ stands for air, 0_2, N_2 and F_{12}). The convective heat transfer coefficient is measured with gas/liquid combination ratios one-to-three, one-to-one and three-to-one. The heat transfer data have been correlated by dimensional analysis. The data have been compared with the empirical correlations and analytical expression and a good correlation is obtained over the range of the Rayleigh number from 2.0×10^4 to 4.0×10^7. Additionally, an empirical correlation relationship is proposed to evaluate the efficiency of convection and the results for gas/liquid combination in the combination ratio one-to-three and three-to-one are presented.

2. EXPERIMENTAL ARRANGEMENT AND PROCEDURE

The general description of the apparatus used in this investigation has been described elsewhere [9-12]. However, a brief description of the equipment is furnished here for expedience. The hot wire cell used in the present study was made from a copper cylinder (diameter = 53.0 mm) with a fine platinum wire (diameter = 0.025 mm) stretched along its axis. The hot wire cell in series with a standard resistor was placed in one arm of a Wheatstone bridge and could be positioned at any angle between the vertical and horizontal orientations. Electric fields in the cell were created by an aplied electric potential (dc and ac) between the cylinder and the wire which was earthed. In order to obtain the heat transfer data, the platinum wire was calibrated as a platinum resistance thermometer. The heating current was supplied from a constant current source, while the surrounding temperature was maintained constant in a constant temperature bath. The bridge was kept balanced for any experimental situation.

3. RESULT AND DISCUSSION

The results for the fluid combination air/water, oxygen/water, nitrogen/water and Freon-12/water are presented in Fig. 1a, 1b, 1c, and 1d respectively. In the case of combination ratio one-to-three (curve 1, Figs. 1a-d) the ENN increases slightly with increase in electric field and then decreases gradually as the field is further increased and with continued increases in electric field, it becomes negative and follows a trend similar to that observed in water. For the combination ratio one-to-one (curve 2, Figs. 1a-d) the ENN increases with increase in electric field, reaches maximum value and then decreases

again and reaches a zero value as the field is further increased. A similar trend is noticed for the combination ratio three-to-one (curve 3, Figs. 1a-d), but the increase in ENN is maximal as observed in this case.

For the three cases considered above, quite a different flow regime exists in the two fluid layers considered. The highest ENN for the system air/water, 0_2/water, N_2/water and F_{12}/water is achieved when the combination ratio is of the order of three-to-one, as the circulating gas (air, 0_2, N_2 and F_{12}) flow is scarcely retarded (by virtue of the low viscosity and therefore impinges on the water surface with a higher velocity. The smallest ENN corresponds to curve 1 in Figs. 1a-d, since the water-side ENN is hampered by the secondary flow cell.

The results for the fluid combination air/ethyl alcohol, oxygen/ethyl alcohol, nitrogen/ethyl alcohol, Freon-12/ethyl alcohol are presented in Figs. 2a-d respectively. In each case, the ENN increases with increase in electric field, reaches a saturation value and then decreases again as the field is further strengthened. The ENN manifests itself in the formation of a maximum value at the gas/liquid ratio of three-to-one (curve 3 in Figs. 2a-d) and decreases gradually with increasing liquid layer thickness (curves 2 and 3, figs. 2a-d).

The above mentioned phenomena are possibly due to the following fact. The thermal conductivity of the liquid filled space (ethyl alcohol) is higher than the gas-filled space (air, 0_2, N_2, F_{12}). The influence of the clockwise eddy in the gas-filled space increases with electric field. The increase in ENN is large as the clockwise secondary eddy in the liquid filled space increases the influence of the counter-clockwise eddy. As the influence of this secondary eddy increases with electric field, the change in the ENN spreads slowly from the edge of the gas/liquid interface to the bottom of the tube. The bottom corresponds to a stagnation point and the ENN at the bottom is lower than at the edge of the gas/liquid interface. The ENN is gradually increasing with electric field exhibiting the phenomena of saturation as displayed in each case.

Figure 3a shows the Nusselt number for air/silicon oil combination. In the lowe regime, Nusselt number decreases slightly with increasing electric field, and the decreas in the ratio three-to-one (curve 3) is smaller than the ratio one-to-three (curve 1). Nusse number reaches the minimum value after an electric field of about 1 (V/cm) but th Nusselt number then increases with increasing electric field and reaches a saturatio value as observed in each case. The rate of increase in the ratio three-to-one is als higher than the ratio one-to-three. In the higher regime, the difference in the Nusse number between the two ratios also increases. This may be attributed to the fact tha owing to the high viscosity of the silicon oil, convection in the silicon oil filled space i less efficient, and this in turn, reduces the rate of ENN in the ratio one-to-three. In th ratio one-to-one, the ENN rate is slightly higher than one-to-three, since the silicon o filled space reduces from 75% to 50%.

Figures 3b and 3c show the results for the ENN for fluid combinatio oxygen/silicon oil and nitrogen/silicon oil. The minimum in ENN at lower electric fie is negligible, but the ENN increases significantly as the field is gradually increased. Th phenomenon of saturation is also clearly indicated in both case. At higher electric fie

strength, the ENN decreases and approaches towards a zero value. The difference in ENN among the three ratios is significantly wide in the high field region, while in the low field region, difference is quite small. Also, the ENN decreases slightly with increasing silicon oil level. The reason may be due to the following:

i) The circulation of the secondary eddy due to electric field is enhanced by free convective motion.

ii) The free convective motion in the highly viscous fluid is less efficient than low viscous fluid.

The results for the fluid combination Freon-12/silicon oil is shown in Fig. 3d. As seen in the figure, the minimum in ENN observed in this case is negligible. The ENN increases with increasing electric intensity in each combination ratios, the highest increase is observed for the ratio three-to-one. In this case, F-12 is the lighter fluid at the top, convering 75% of the cylinder, while the ENN decreases as the ratios decrease, the minimum in ENN is observed in the ratio one-to-three. The results reveal that, for a given electric field strength, the most intensive ENN can be achieved with the system F_{12}/silicon oil, because of a very intensive convective flow in both layers.

For the air/kerosene combination, the development of the electrically induced convection from pure buoyancy driven flow is presented in Fig. 4a. The results for various air/kerosene combination ratios indicate an increase in EN with an increasing electric field, it then reaches a saturation value and then decreases again as the field is further strengthened. However, a slight inhibition in convection is noted at a lower field regime, especially for the combination ratio one-to-three (curve 1) and one-to-one (curve 2). This is attributed to the fact that at lower field regime, the secondary eddy is weak and occupies a small area, while the electrophoretic force arising from the free charges in the fluid medium is dominating and causing an inhibition at lower regime. As the field is increased gradually, the secondary flow cell grows in strength and volume and this in turn, increases the r.m.s. velocity of the convection. The resulting flow cells below and above the interface have quite identical shapes and thus enhances the ENN significantly, while the decrease at higher electric field is due to Joule heating.

The results for the fluid combination 0_2/kerosene, N_2/kerosene and F_{12}/kerosene are presented in figs. 4b-d respectively. In 0_2/kerosene and N_2/kerosene combination, a sharp rise in ENN is noted. This is due to the fact that the roll cell situated in the N_2-filled and 0_2-filled space grows in strength with increasing electric field. Due to the more powerful convective motion, the ENN is also increased, as observed in figs. 4b and 4c respectively.

The increase in ENN in F_{12}/kerosene is noteworthy. The increase in ENN in each combination ratio is almost linear and then reaches a saturation value. The sharp increase in ENN in various combination ratios may be associated with the strong convective motion arising from the freon-filled space and kerosene-filled space.

In the presence of electric field, the efficiency of convection (E0C) can be calculated using the following relationship [10, 13-15]

$$Y = - \frac{}{} \qquad (1)$$

where h_f is the free convection heat transfer coefficient and h_{el} is the electroconvective heat transfer coefficient. The E0C for the two fluid combinations (gas/liquid) are presented in Tables I-III, in the combination ratio one-to-three and three-to-one respectively.

The results for the fluid combination Δ/water are presented in Table I (Δ = air, 0_2, N_2 and F_{12}). As seen in the Table, the efficiency of convection increases with increase in electric intensity, reaches a maximum value and then decreases again as the field is further intensified. With continued intensification, it reaches a zero value and then becomes negative, as seen in most of the cases. A zero value implies an absence of convection, while a negative value implies a suppression of the free-convection by electroconvection. The E0C follows a trend similar to that found in Δ/water combination. Also, in all cases of fluid combination, the E0C in the combination ratio three-to-one. As seen in the Tables (I-III), the maximum efficiency corresponds to the combination ratio three-to-one. The highest efficiency obtained for the combination ratio F_{12}/silicon oil is 71%, and seems to be the most suitable fluid combination for convection.

The increase in efficiency in the combination ratio three-to-one as compared to one-to-three may be associated with the viscosity of the fluids. Convection in low viscuous fluids (air, 0_2, N_2, F_{12}) are more efficient than highly viscuous fluids (water, ethyl alcohol, silicon oil). Thus, for combination ratios three-to-one, 75% of the cylinder is filled with highly viscuous fluids, whereas in the combination ratio one-to-three, 25% of the cylinder is filled with highly viscuous fluids. The larger volumes for highly viscuous fluids in the ratio three-to-one enhances the convection as compared to the smaller volumes for low viscuous fluids in the ratio one-to-three.

TABLE I: The E0C in air/water, 0_2/water, N_2/water and F_{12}/water combination in combination ratio one-to-three and three-to-one respectively

$E_s x10^{-5}$ (V/cm)	Air/Water		Oxygen/Water		Nitrogen/Water		Freon-12/Water	
	1 : 3	3: 1	1 : 3	3 : 1	1 : 3	3 : 1	1 : 3	3 : 1
	Y(%)	Y(%)	Y(%)	Y(%)	Y(%)	Y(%)	Y(%)	Y(%)
0.26	12.0	11.0	17.0	18.0	10.0	2.0	1.0	2.0
0.52	19.0	20.0	25.0	23.0	16.0	6.0	3.10	4.0
0.78	26.0	25.0	36.0	31.0	29.0	14.0	5.0	6.0
1.04	33.0	29.0	45.0	42.0	38.0	21.0	8.0	10.0
1.30	39.0	37.0	52.0	50.0	27.0	33.0	12.0	14.0
1.56	45.0	46.0	57.0	55.0	18.0	42.0	22.0	24.0
1.82	36.0	51.0	60.0	57.0	9.0	50.0	33.0	36.0
2.08	20.0	55.0	53.0	60.0	0	40.0	38.0	40.0
2.32	11.0	59.0	41.0	62.0	-7.0	27.0	44.0	46.0
2.60	9.0	63.0	30.0	64.0	-15.0	18.0	45.0	48.0
2.86	0	65.0	19.0	65.0		8.0	44.0	51.0
3.12	-7.0	66.0	11.0	67.0		0	41.0	54.0
3.38	-15.0	67.0	0.0	68.0		-11.0	32.0	58.0
3.64	-24.0	67.0	-8.0	68.0		-20.0	17.0	60.0
3.90		67.0	-15.0	69.0			4.0	63.0
4.16		66.0	-26.0	69.0			0	65.0
4.42		65.0		68.0			-3.0	67.0
4.68		64.0		67.0			-5.0	68.0
4.94		62.0		65.0			-9.0	69.0
5.20		60.0		63.0			-13.0	69.0
5.72				61.0			-18.0	70.0
6.24				57.0			-24.0	71.0
6.76				51.0				66.0
7.28				44.0				57.0
7.80				38.0				44.0
8.32				30.0				31.0
8.84				21.0				11.0
9.36				15.0				0
9.88								-5.0
10.40								-8.0
11.44								-12.0
12.48								-18.0
13.52								

TABLE II :The E0C in air/ethyl alcohol , 0_2/ethyl alcohol, N_2/ethyl alcohol and F_{12}/ethyl alcohol combination in combination ratio one-to-three and three-to-one respectively.

$E_s x10^{-5}$ (V/cm)	Air/Ethyl Alcohol		0_2/Ethyl Alcohol		N_2/Ethyl Alcohol		F_{12}/Ethyl Alcohol	
	1 : 3	3: 1	1 : 3	3 : 1	1 : 3	3 : 1	1 : 3	3 : 1
	Y(%)	Y(%)	Y(%)	Y(%)	Y(%)	Y(%)	Y(%)	Y(%)
0.26	2.0	2.0	2.0	1.0	1.0	2.0	1.0	2.0
0.52	10.0	11.0	12.0	9.0	4.0	6.0	11.0	13.0
0.78	30.0	33.0	30.0	19.0	9.0	12.0	18.0	21.0
1.04	40.0	45.0	33.0	26.0	17.0	20.0	28.0	30.0
1.30	45.0	47.0	35.0	41.0	28.0	30.0	33.0	36.0
1.56	46.0	50.0	39.0	36.0	33.0	35.0	36.0	40.0
1.82	49.0	53.0	44.0	42.0	38.0	40.0	40.0	44.0
2.08	48.0	59.0	47.0	47.0	42.0	43.0	47.0	51.0
2.34	47.0	61.0	51.0	52.0	44.0	45.0	49.0	56.0
2.60	45.0	63.0	50.0	54.0	46.0	47.0	51.0	60.0
2.86	40.0	66.0	48.0	57.0	38.0	48.0	52.0	63.0
3.12	31.0	68.0	47.0	58.0	27.0	50.0	53.0	66.0
3.38	18.0	69.0	44.0	60.0	18.0	51.0	53.0	68.0
3.64	5.0	68.0	40.0	62.0	6.0	53.0	52.0	70.0
3.90	0	68.0	33.0	64.0	0	54.0	50.0	71.0
4.16		66.0	19.0	67.0		55.0	45.0	71.0
4.42		65.0	11.0	70.0		51.0	39.0	71.0
4.68		63.0	4.0	71.0		40.0	28.0	70.0
4.94		59.0	0	71.0		28.0	17.0	70.0
5.20		52.0		71.0		19.0	10.0	68.0
5.46		41.0		70.0		12.0	0.0	64.0
5.72		30.0		67.0		6.0		61.0
5.98		19.0		64.0		2.0		55.0
6.24		10.0		59.0		0		49.0
6.56		4.0		48.0				41.0
6.76		0.0		39.0				35.0
7.02				27.0				28.0
7.28				18.0				21.0
7.54				9.0				15.0
7.8				0				11.0
8.84								6.0
9.36								2.0

TABLE III: The E0C in air/silicon oil, 0_2/silicon oil, N_2/silicon oil and F_{12}/silicon oil combination in combination ratio one-to-three and three-to-one respectively.

$E_x x10^{-5}$ (Vcm)	Air/Silicon Oil		0_2/ Silicon Oil		N_2/ Silicon Oil		F_{12}/ Silicon Oil	
	1 : 3	3: 1	1 : 3	3 : 1	1 : 3	3 : 1	1 : 3	3 : 1
	Y(%)	Y(%)	Y(%)	Y(%)	Y(%)	Y(%)	Y(%)	Y(%)
0.52	0.5	1.0	2.0	3.0	1.0	2.0	2.5	3.0
1.04	1.0	1.0	3.0	9.0	1.0	10.0	3.0	4.0
1.56	2.0	1.5	4.0	19.0	2.0	14.0	4.0	5.0
2.08	3.0	2.0	5.0	30.0	3.0	18.0	5.0	6.0
2.34	4.0	5.0	6.0	41.0	4.0	22.0	7.0	8.0
2.60	6.0	9.0	7.0	50.0	5.0	27.0	9.0	11.0
2.86	7.0	13.0	9.0	61.0	5.0	33.0	11.0	13.0
3.12	9.0	18.0	12.0	63.0	6.0	38.0	14.0	16.0
3.38	11.0	22.0	14.0	64.0	7.0	40.0	17.0	20.0
3.64	12.0	27.0	17.0	64.0	9.0	43.0	20.0	23.0
3.90	14.0	33.0	19.0	65.0	12.0	45.0	24.0	27.0
4.16	16.0	38.0	21.0	65.0	16.0	46.0	28.0	31.0
4.42	19.0	43.0	24.0	64.0	18.0	46.0	32.0	35.0
4.68	21.0	51.0	27.0	63.0	20.0	45.0	36.0	39.0
4.94	25.0	55.0	31.0	62.0	23.0	43.0	39.0	42.0
5.20	27.0	54.0	35.0	60.0	25.0	40.0	44.0	46.0
5.72	29.0	52.0	39.0	55.0	27.0	36.0	48.0	50.0
6.24	32.0	45.0	41.0	44.0	29.0	32.0	52.0	55.0
6.76	33.0	33.0	44.0	39.0	31.0	28.0	55.0	60.0
7.28	35.0	18.0	47.0	30.0	33.0	24.0	58.0	65.0
7.80	37.0	11.0	50.0	19.0	35.0	19.0	61.0	70.0
8.32	39.0	2.0	52.0	9.0	36.0	13.0	63.0	71.0
8.84	41.0	0	54.0	5.0	38.0	9.0	66.0	69.0
9.36	42.0		55.0	2.0	39.0	5.0	65.0	68.0
9.88	43.0		56.0	0	40.0	2.0	64.0	66.0
10.40	43.0		56.0		41.0	0	63.0	63.0
11.44	44.0		56.0		41.0		61.0	60.0
12.48	44.0		54.0		37.0		55.0	56.0
13.52	42.0		49.0		34.0		48.0	49.0
14.04	40.0		42.0		30.0		40.0	41.0
14.56	35.0		35.0		20.0		31.0	33.0
15.60	31.0		29.0		11.0		20.0	25.0

The Nusselt number is plotted as a function of Rayleigh number for fluid combination air/water, oxygen/ethyl alcohol and Freon-12/silicon oil and the results are presented in figs. 5a-c respectively. Also plotted in the figures are the various empirical relations and analytical expression available for free convection. Curve 1 in figs. 5a-c is the predicated correlation proposed by Warrington and Pwe [16] and is given by

$$\left(Nu_{el}\right)_D = m\left(Ra_D\right)^n \tag{2}$$

Curve 2 in figs. 5a-c is the predicated correlation proposed by Al-Arabi and Khamis [17] and is given by

$$\left(Nu_D\right) = (0.58)\left(Gr_D\right)^{-\frac{1}{2}}\left(Ra_D\right)^{\frac{1}{4}} \tag{3}$$

while curve 3 in Figs. 5a-c resulted from the predicated correlation proposed by Churchill and Chu [18]. For horizontal cylinder

$$Nu_D = \left\{0.60 + 0.387\left(Ra_D\right)^{\frac{1}{6}}\left[1+\left(\frac{0.559}{\mathrm{Pr}}\right)^{\frac{9}{16}}\right]\right\}^2 \tag{4}$$

The analytical expression available for free convection [19] is given by

$$(Nu)_D = 0.637\left(Ra_D\right)^{\frac{1}{4}}\left[1+\frac{0.861}{\mathrm{Pr}}\right]^{-\frac{1}{4}} \tag{5}$$

and the result is presented in curve 4 of fig. 5a-c respectively.

The predicated relations and the analytical expression could fit the experimental data well, the goodness of fitness was achieved by adjusting the index of the Rayleigh number in various relations. An excellent agreement ($\approx$ 85%) with experiment was achieved for the fluid combination oxygen/ethyl alcohol and F_{12}/silicon oil, whereas in the case of air/water combination, the experiential values predicted slightly higher Nu_{el} number than the predicted correlations for Ra> 1.75×10^5. Table IV summarizes the index of the Rayleigh number in absence and in presence of electric field. As seen in the table, the index of the Rayleigh number is increased in presence of an electric field, implying the fact that the E0C increases when an electric field is applied to free convention motion.

TABLE IV A comparison of the exponent of the Rayleigh number for various gas/liquid combinations (air/water, 0_2/ethyl alcohol, F_{12}/silicon oil) in absence and in presence of electric fields.

Curves in Figs. 5a-c	Exponent of Rayleigh Number			
	When E = 0	When E ≠ 0		
		Air/Water	0_2/Ethyl alcohol	F_{12}/Silicon Oil
1	0.171	0.42	0.46	0.51
2	0.25	0.43	0.45	0.51
3	0.17	0.23	0.27	0.30
4	0.25	0.36	0.42	0.47

5. CONCLUSION

i) ENN in gas/liquid combination system has been presented. They include the combination ratio one-to-three, one-to-one and three-to-one respectively.

ii) ENN in the fluid combinations Δ/water, Δ/ethyle alcohol, Δ/silicon oil and Δ/kerosene (Δ = air, 0_2, N_2, F_{12}) increases with increasing electric intensity and approaches a saturation value.

iii) With continued electric intensification, ENN decreases and approaches zero value, as may be noticed in most of the cases.

iv) ENN in the combination ratio three-to-one is found to be higher than the ratio one-to-three.

v) The E0C in various fluid combinations also increases with increasing electric intensity, reaches a maximum value and then approaches zero value as the electric intensity is further increased. A zero value of efficiency implies an absence of convection, while a negative value (as may be observed in some cases) implies a suppression of free convection by electroconvection. The maximum efficiency obtained in the fluid combination F_{12}/silicon oil in the combination ratio three-to-one is 71% , and is found to be the most suitable combination for convection.

vi) The experimental data agrees well with the predicted relations and analytical expression available for free-convection. An agreement of about 85% was obtained in most of the cases. The agreement was obtained by changing the index of the Rayleigh number, which oscillates between 0.23 and 0.51 in all cases of fluid combinations.

ACKNOWLEDGEMENT

The experiment part of the work described in this paper were carried out at the Physics Department, Clarkson University, Potsdam, New York, U.S.A. The authors are grateful to Professor S. Arajs for providing the laboratory facility and for supervising the experimental data collection.

Research grant awarded by Abubakar Tafawa Balewa University of Technology, Bauchi, Nigeria in connection with the preparation of this paper is also gratefully acknowledged.

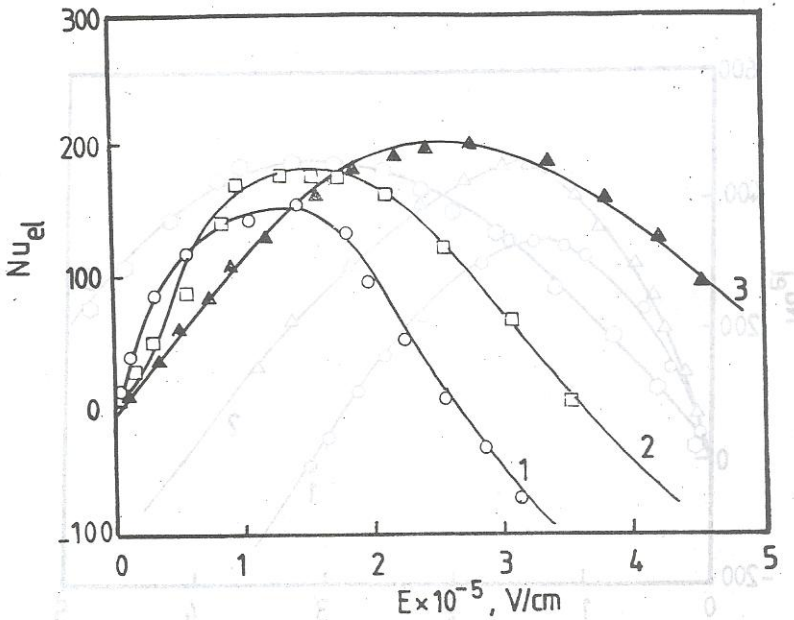

Fig. 1a Electric Nusselt number variation with applied electric field intensity for air/water combination in the combination ratio.

1. one-to-three
2. one-to-one
3. three-to-one

Horizontal cylinder $T_d = 8.8^0C$, P_{air} = 40-5 cm Hg.

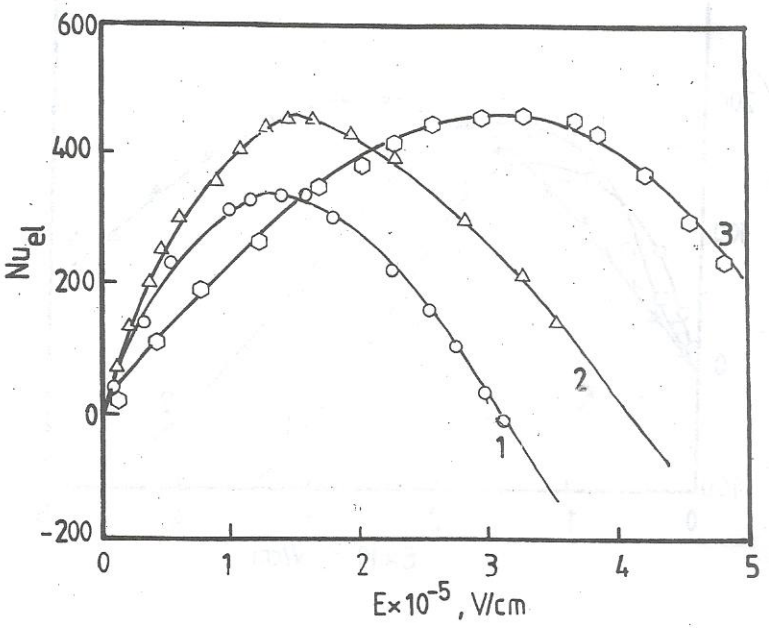

Fig. 1b **Electric Nusselt number variation with applied electric field intensity for 0_2/water combination in the combination ratio**

1. one-to-three
2. one-to-one
3. three-to-one

Horizontal cylinder, $T_d = 9.0^0C$, $P0_2 = 41.0$ cm Hg.

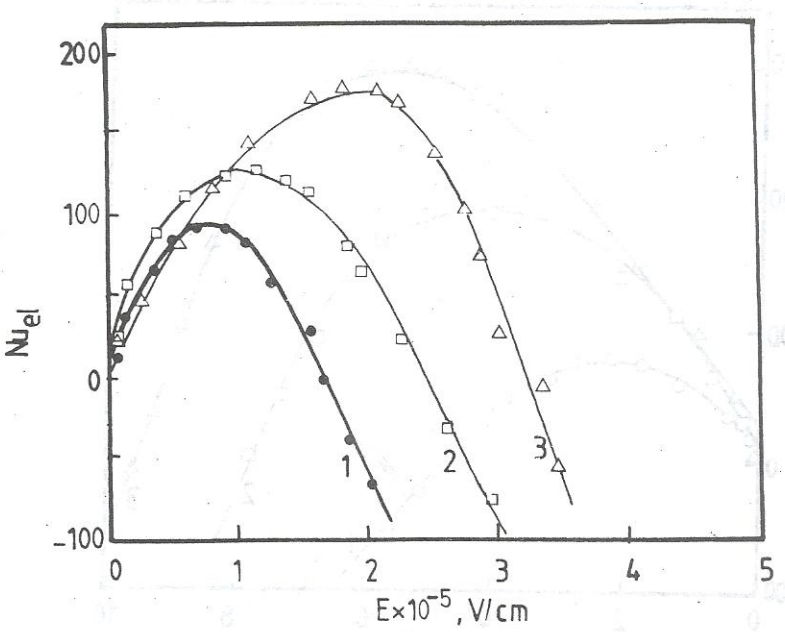

Fig. 1c Electric Nusselt number variation with applied electric field intensity for N_2/water combination in the combination ratio

1. one-to-three
2. one-to-one
3. three-to-one

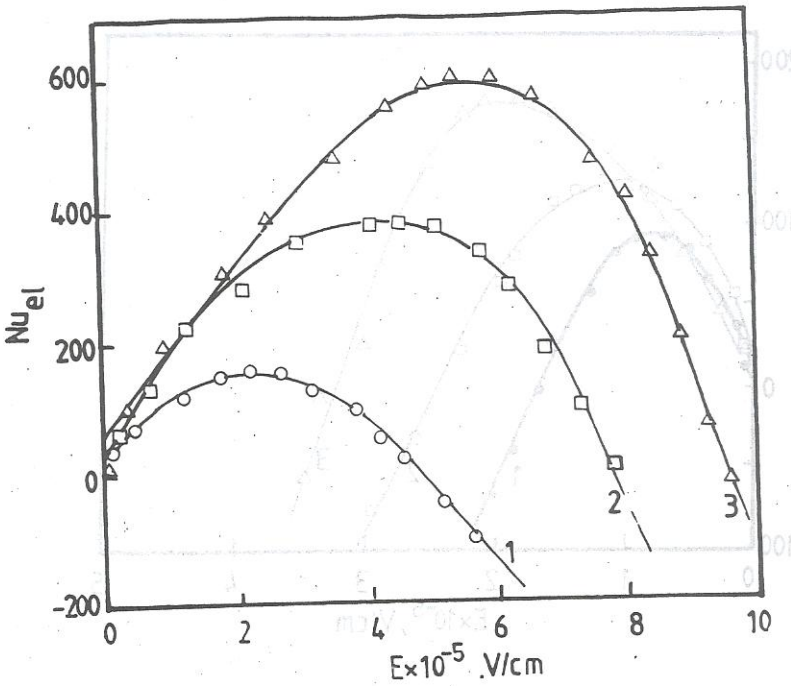

Fig. 1d Horizontal cylinder, $T_d = 7.5^0C$, $PN_2 = 35.0$ Hg.
Electric Nusselt number variation iwht applied electric field intensity for F_{12}/water combination in the combination ratio
1. one-to-three
2. one-to-one
3. three-to-one
Horizontal cylinder, $T_d = 12.0^0C$, $PF_{12} = 45.0$ cm Hg.

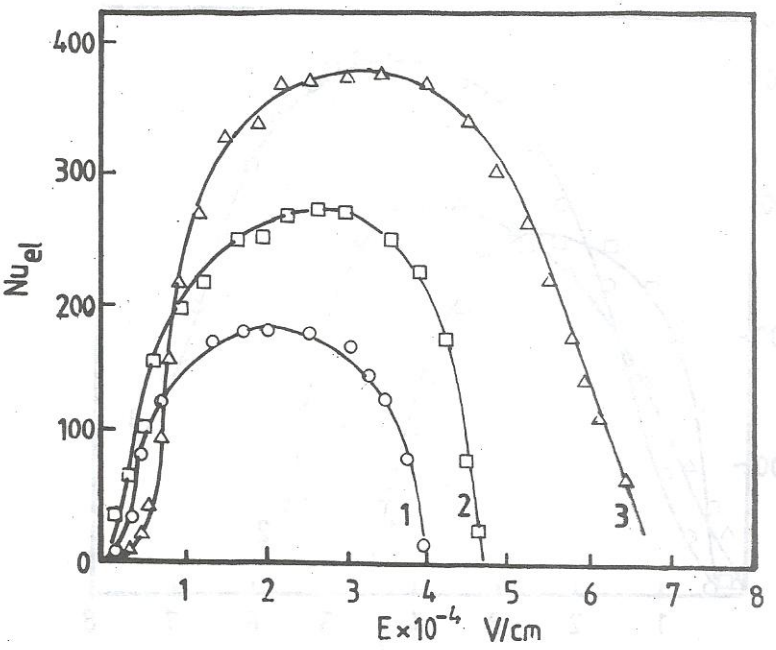

Fig. 2a **Electric Nusselt number variation with applied electric field intensity for air/ethyl alcohol combination in the combination ratio**

1. one-to-three
2. one-to-one
3. three-to-one

Horizontal cylinder, $T_d = 7.1^0C$, $P_{air} = 42.0$ cm Hg.

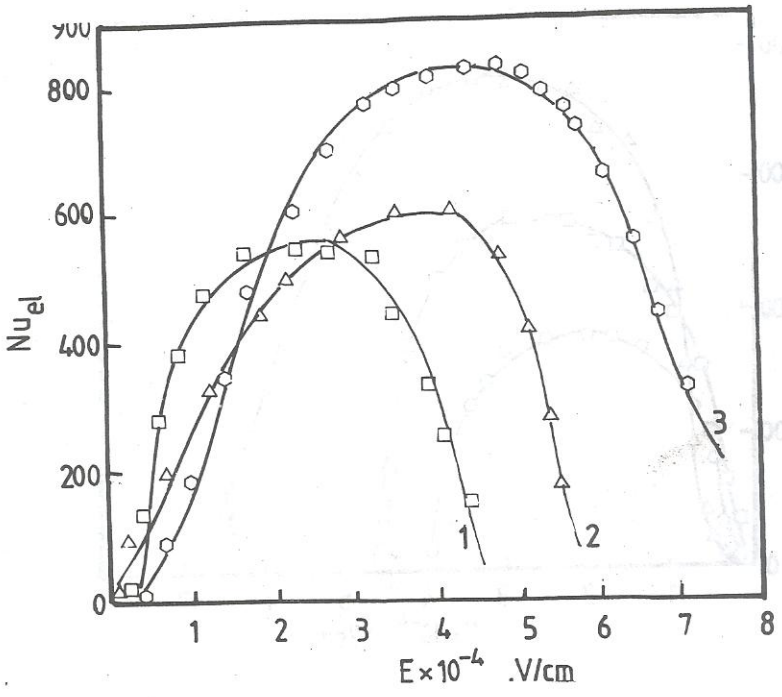

Fig. 2b Electric Nusselt number variation with applied electric field intensity for 0_2/ethy alcohol combination in the combination ratio

1. one-to-three
2. one-to-one
3. three-to-one

Horizontal cylinder, $T_d = 7.0^0C$, $PN_2 = 32.0$ cm Hg.

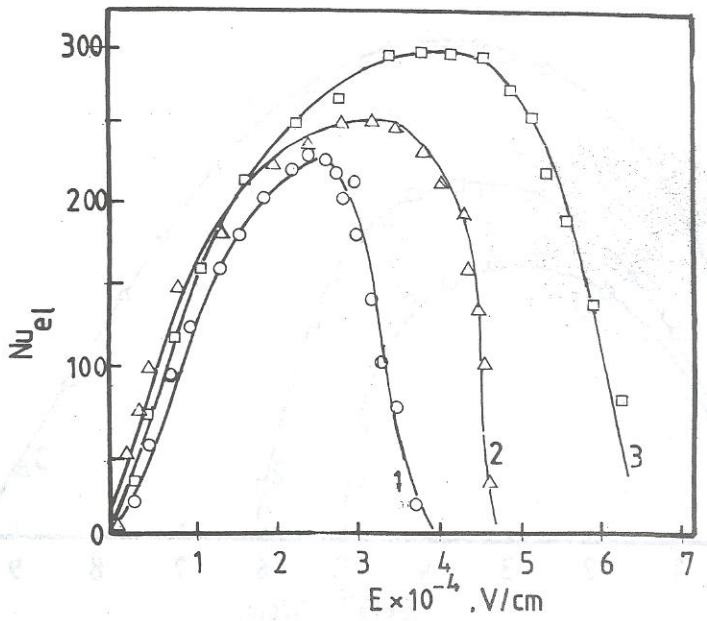

Fig 2c Electric Nusselt number variation with applied electric field intensity for N_2/ethy alcohol combination in the combination ratio

1. one-to-three
2. one-to-one
3. three-to-one

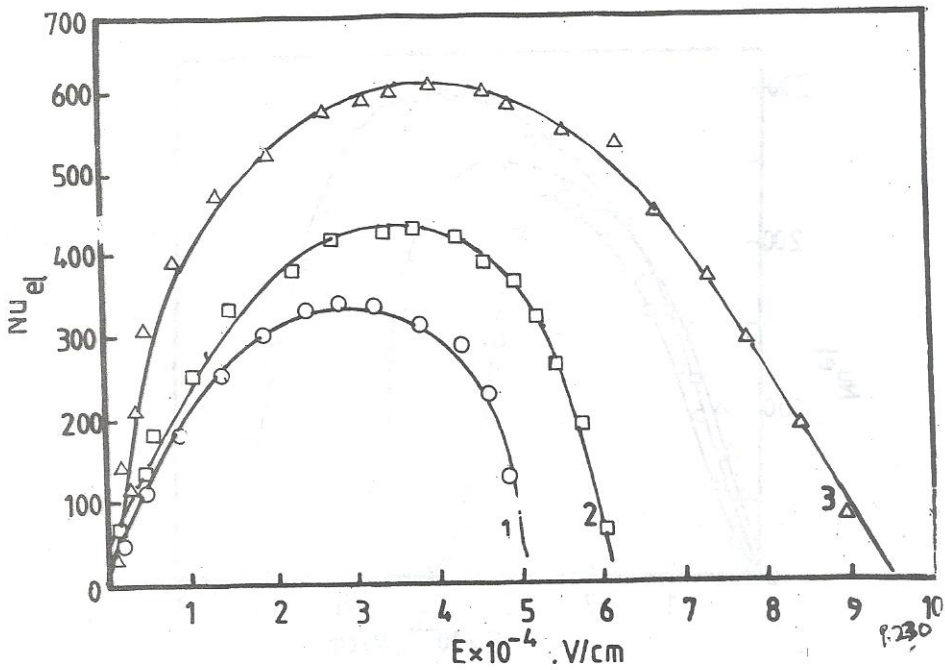

Fig. 2d Electric Nusselt number variation with applied electric field intensity for F_{12} ethy alcohol combination in the combination ratio
1 one-to-three
2 one-to-one
3 three-to-one
Horizontal cylinder, T_d = 12.0°C, PF_{12} = 46.0 cm Hg.

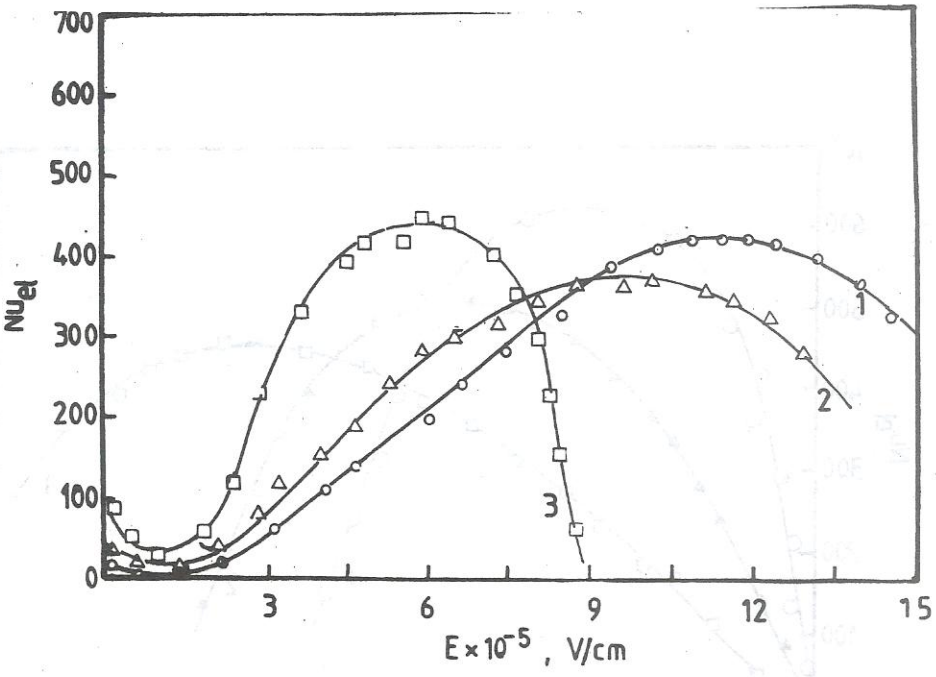

Fig. 3a **Electric Nusselt number variation with applied electric field intensi for air/silicon oil combination in the comgination ratio**

1. one-to-three
2. one-to-one
3. three-to-one

Horizontal cylinder, $T_d = 12.0^0C$, $P_{air} = 45.0$ cm Hg.

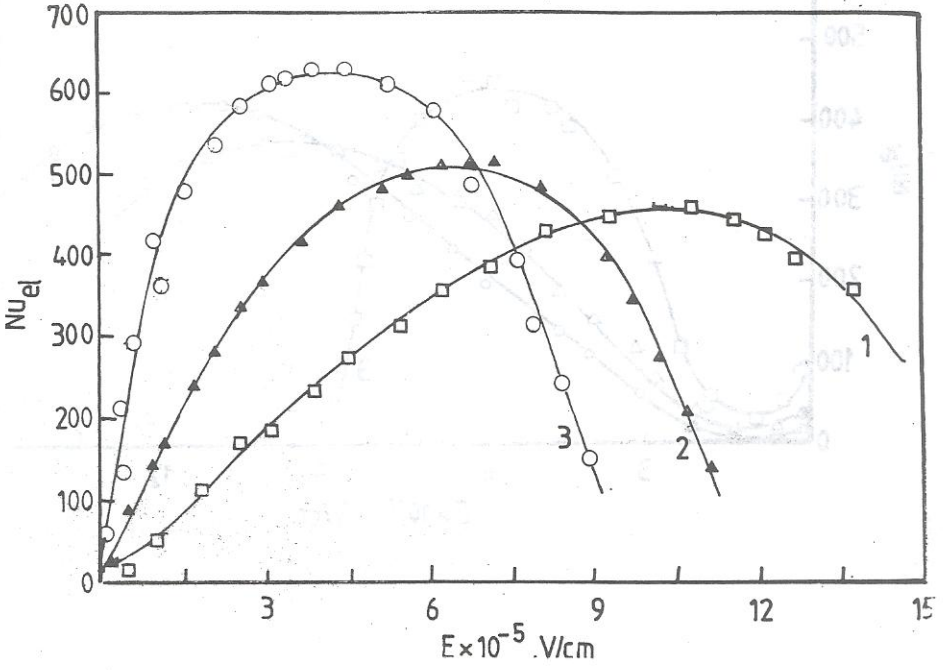

Fig. 3b Electric Nusselt number variation with applied electric field intensity for 0_2 silicon oil combination in the combination ratio
1. one-to-three
2. one-to-one
3. three-to-one
Horizontal cylinder, T_d 12.5°C, $P0_2$ 44.0 cm Hg.

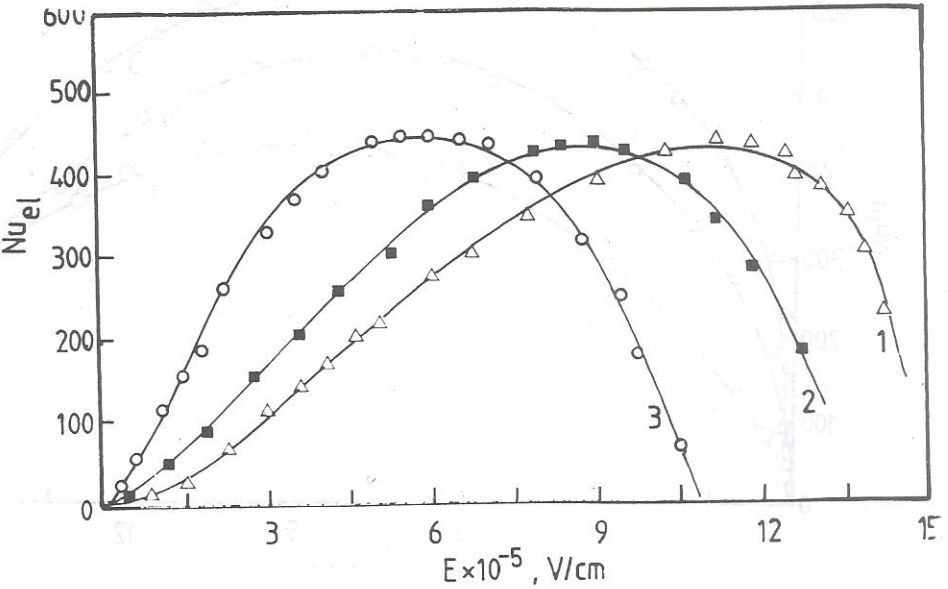

Fig. 3c Electric Nusselt number variation with applied electric field intensity for N_2/silicon oil combination in the combination ratio

1. one-to-three
2. one-to-one
3. three-to-one

Horizontal cylinder, $T_d = 12.0^0C$, $PN_2 = 45.0$ cm Hg.

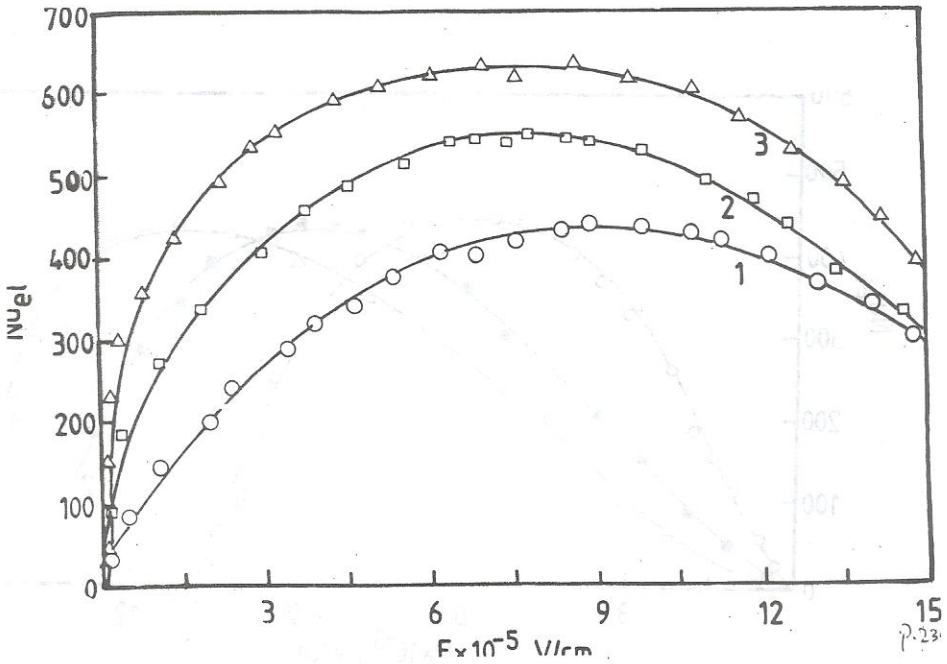

Fig. 3d Electric Nusselt number variation with applied electric field intensity for F_2 silicon oil combination in the combination ratio
1 one-to-three
2. ~~one-to-one~~
3. three-to-one
Horizontal cylinder. T_a 14.0°C, PF_2 49.0 cm Hg.

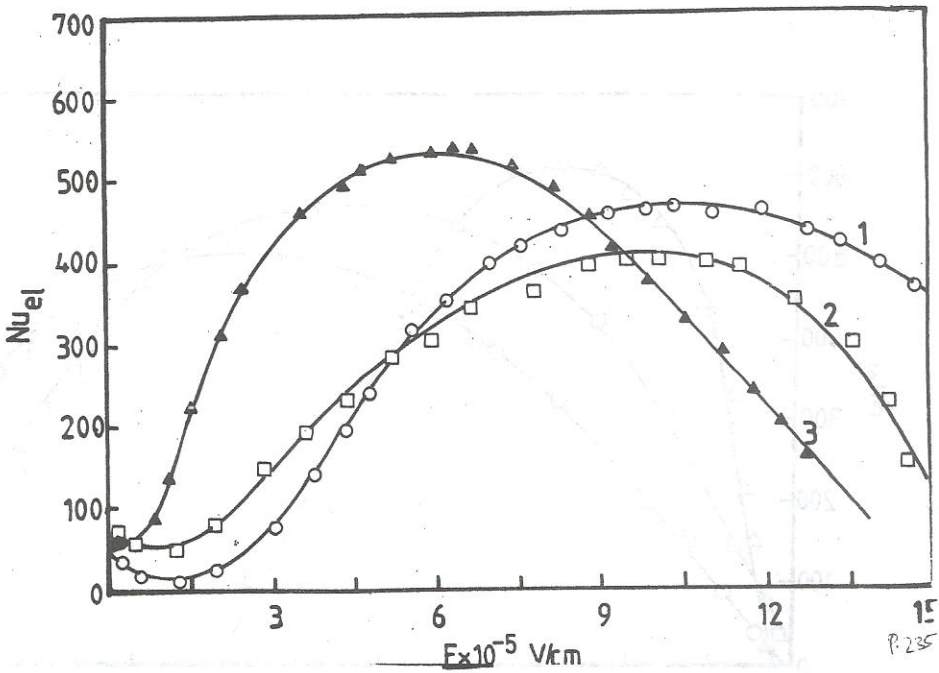

Fig. 4a Electric Nusselt number variation with applied electric field intensity for air/kerosene combination in the combination ratio

1 one-to-three
2. one-to-one
3. three-to-one

Horizontal cylinder, $T_d = 11.5^0C$, $P_{air} = 43.0$ cm Hg.

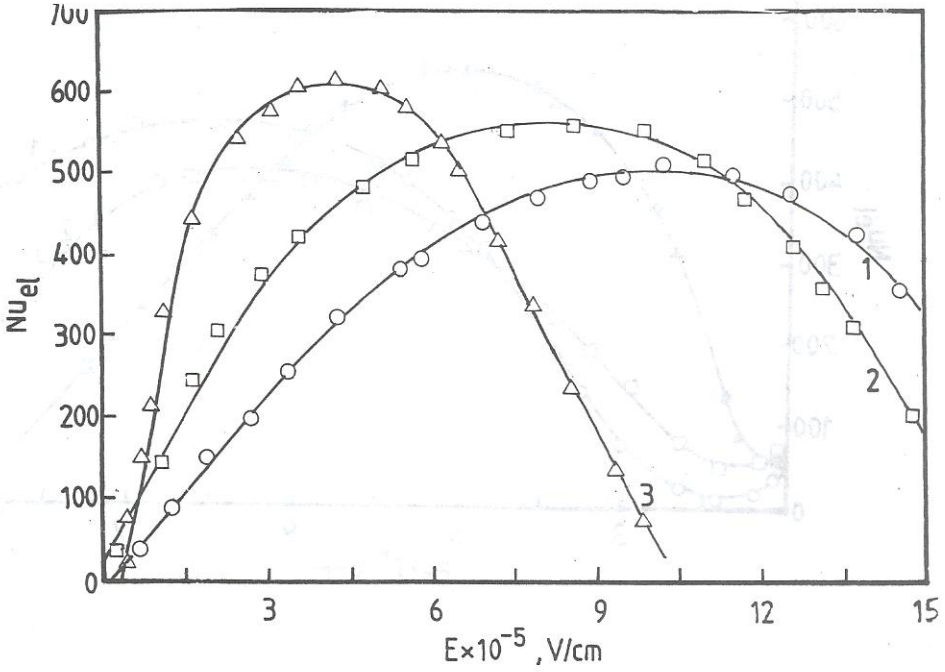

Fig. 4b, Electric Nusselt number variation with applied electric field intensity for 0_2/kerosene combination in the combination ratio

1 one-to-three
2. one-to-one
3. three-to-one

Horizontal cylinder, $T_d = 12.0^0C$, $P0_2 = 50$ cm Hg.

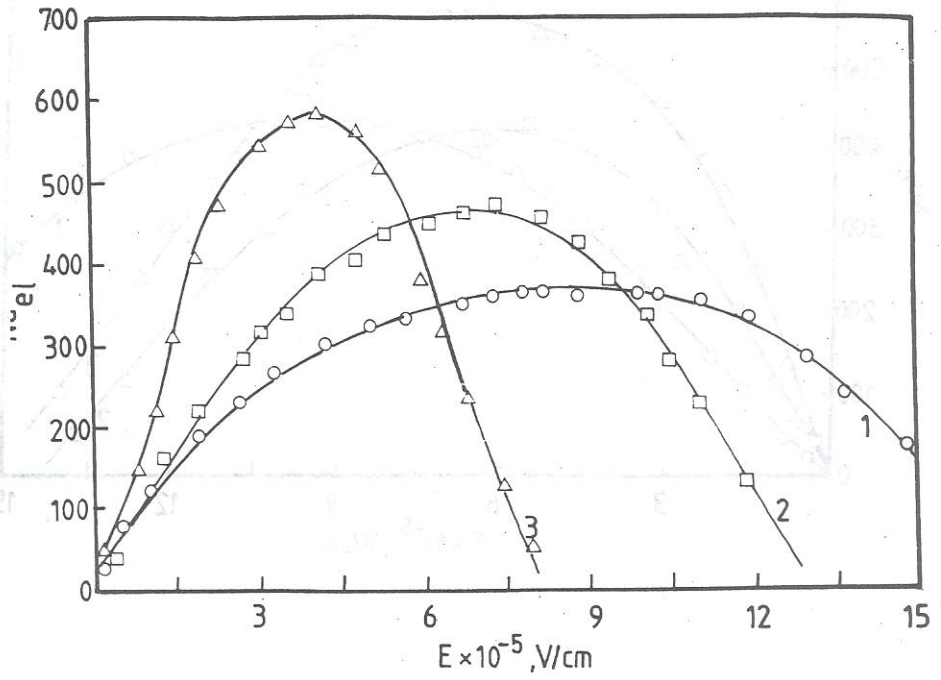

Fig. 4c Electric Nusselt number variation with applied electric field intensity for N_2/kerosene combination in the combination ratio

1 one-to-three
2. one-to-one
3 three-to-one

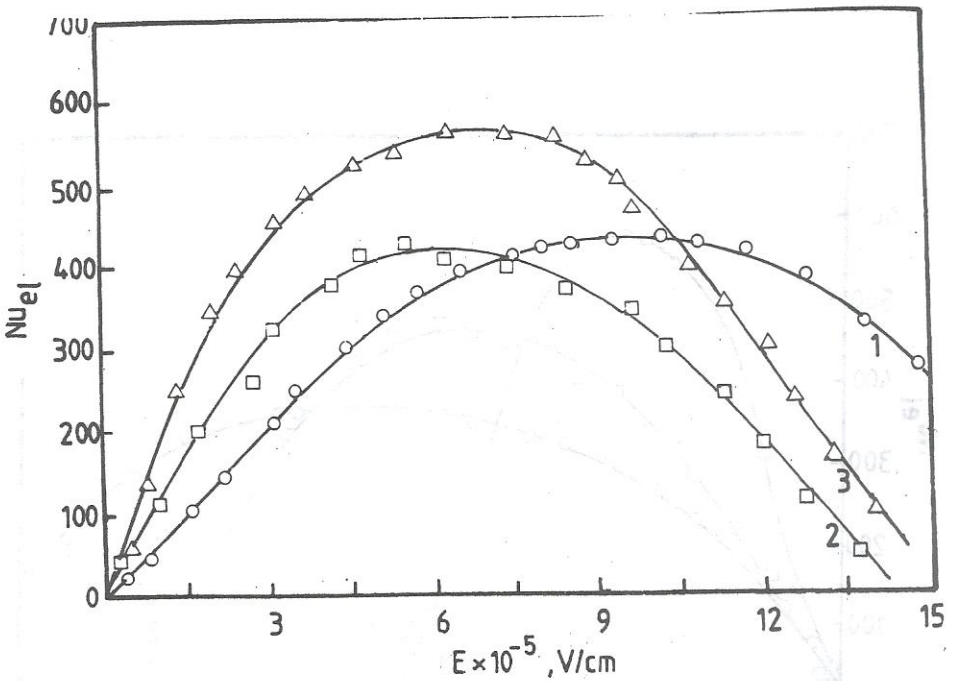

Fig. 4d Electric Nusselt number variation with applied electric field intensity for F_{12}/kerosene combination in the combination ratio

1 one-to-three
2. one-to-one
3 three-to-one

Horizontal cylinder, $T_d = 10.0^0C$, $PN_2 = 40.0$ cm Hg.

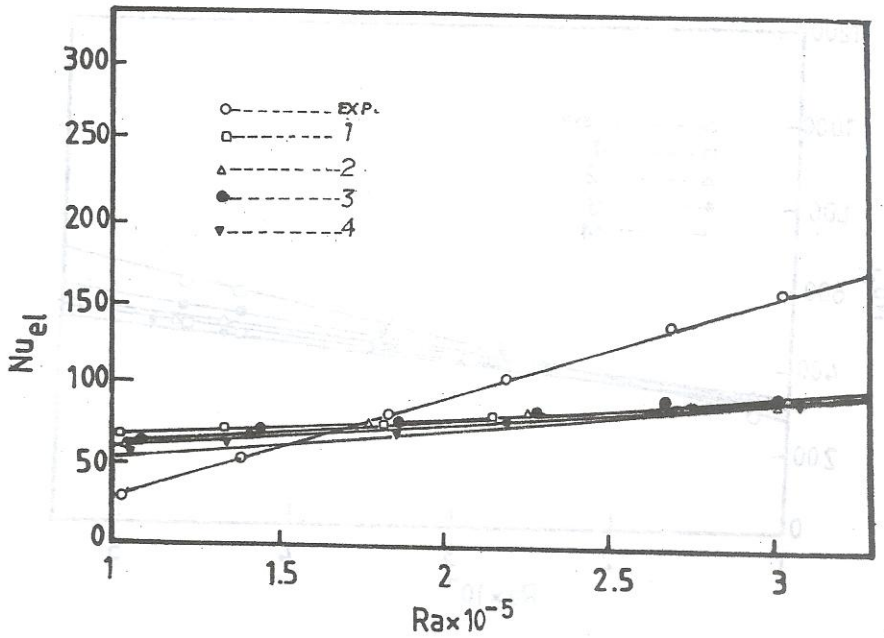

Fig. 5a Correlation of data for electric Nusselt number from a horizontal cylinder.

air/water combination with combination ratio three-to-one

1. $$\left(Nu_{el}\right)_p = 0.30\left(Ra_D\right)^{0.42}$$

2. $$\left(Nu_{el}\right)_p = 0.58\left[\frac{1}{\left(Gr_D\right)^{0.05}}\left(Ra_D\right)^{0.43}\right]$$

3. $$\left(Nu_{el}\right)_p = \left\{0.60 + 0.387\left(Ra_D\right)^{0.23}\left[1+\left(\frac{0.559}{\mathrm{Pr}}\right)^{0.56}\right]^{-0.30}\right\}^2$$

4. $$\left(Nu_{el}\right)_p = 0.637\left(Ra_D\right)^{0.36}\left(1+\frac{0.861}{\mathrm{Pr}}\right)^{-0.25}$$

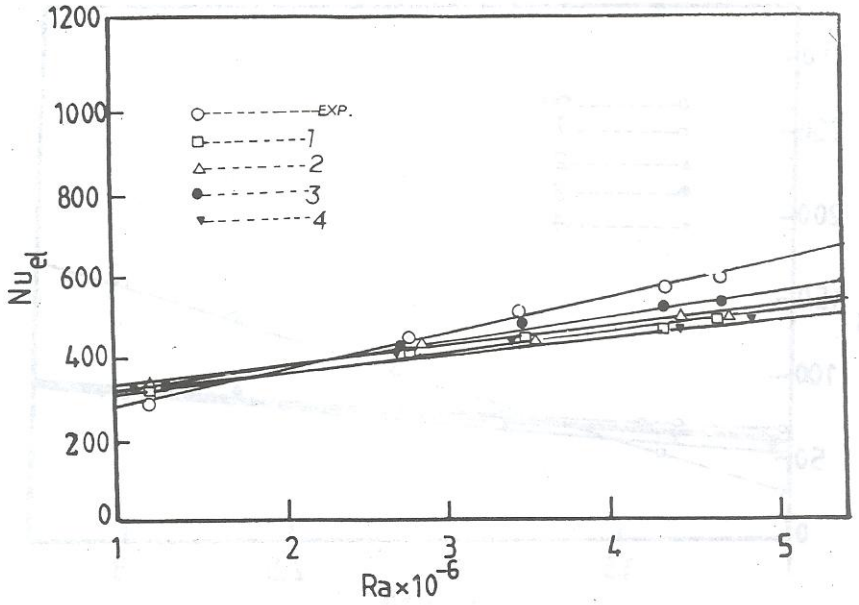

Fig. 5b Correlation of data for electric Nusselt number from a horizontal cylinder.

0_2/ethyl alcohol combination with commination ratio three-to-one

1. $$(Nu_{el})_D = 0.30(Ra_D)^{0.46}$$

2. $$(Nu_{el})_p = 0.58\left[\frac{1}{(Gr_D)^{0.05}}(Ra_D)^{0.45}\right]$$

3. $$(Nu_{el})_D = \left\{0.60 + 0.387(Ra_D)^{0.27}\left[1+\left(\frac{0.559}{\mathrm{Pr}}\right)^{0.56}\right]^{-0.30}\right\}^2$$

4. $$(Nu_{el})_D = 0.637(Ra_D)^{0.42}\left(1+\frac{0.861}{\mathrm{Pr}}\right)^{-0.25}$$

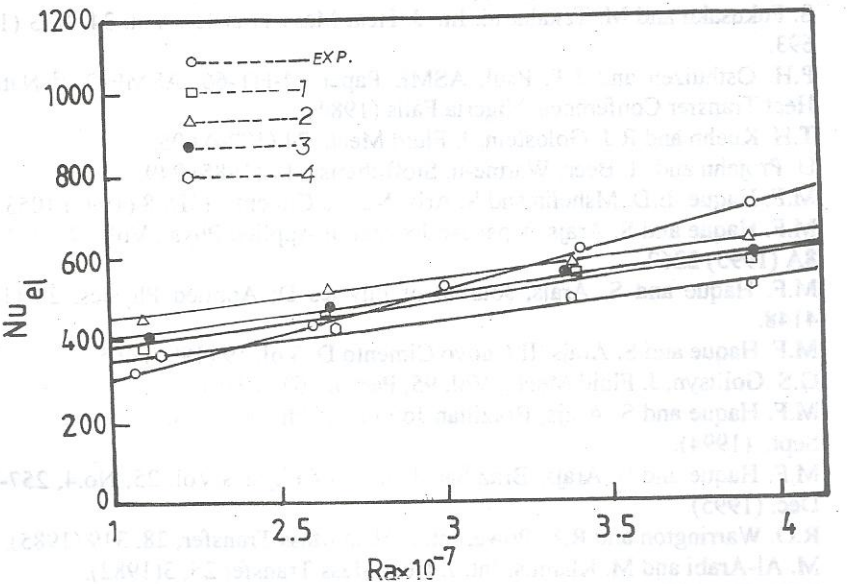

Fig. 5c Correlation of data for electric Nusselt number from a horizontal cylinder.

F_{12}/silicon oil combination with combination ration three-to-one

1 $$\left(Nu_{el}\right)_D = 0.30\left(Ra_D\right)^{0.51}$$

2 $$\left(Nu_{el}\right)_D = 0.58\left[\frac{1}{\left(Gr_D\right)^{0.05}}\left(Ra_D\right)^{0.51}\right]$$

3 $$\left(Nu_{el}\right)_D = \left\{0.60 + 0.387\left(Ra_D\right)^{0.30}\left[1+\left(\frac{0.559}{\mathrm{Pr}}\right)^{0.56}\right]^{-0.30}\right\}^2$$

4 $$\left(Nu_{el}\right)_D = 0.637\left(Ra_D\right)^{0.47}\left(1+\frac{0.861}{\mathrm{Pr}}\right)^{-0.25}$$

REFERENCES

1. H. Senftleben, Phys. Z., 32 (1931) 550.
2. H. Senftleben, Phys. Z., 35 (1934) 661.
3. H. Senftleben and W. Braun, Z. Phys. 102 (1936) 480.
4. G. Ahsman and Dr. Kronig, Appl. Sci. Res. A2 (1950) 235.
5. S. Fukusako and M. Takahashi, Int. J. Heat Mass Transfer, Vol. 34, N. 3 (1991) 693.
6. P.H. Osthuizen and J.T. Paul, ASME Paper 84-HT-66, ASME 22nd National Heat Transfer Conference, Nigeria Falls (1984).
7. T.H. Kuehn and R.J. Goldstein, J. Fluid Mech. 74 (1976) 695.
8. U. Projahn and H. Beer, Warme-u, Stoffubertsr, 19 (1985) 249.
9. M.F. Haque, E.D. Mshelia and S. Arjs, Nuovo Cimento 15D, 8 (1993) 1053.
10. M.F. Haque and S. Arajs, Japanese Journal of Applied Phys., Vol. 34, Pt. 1, No. 8A (1995) 2262.
11. M.F. Haque and S. Arajs, Journal of Physics D; Applied Physics, 28 (1995) 4148.
12. M.F. Haque and S. Arajs, II Nuovo Cimento D, Vol. 19 (1997) 665.
13. G.S. Golitsyn, J. Fluid Mech., Vol. 95, Part 3, 367 (1979).
14. M.F. Haque and S. Arajs, Brazilian Journal of Physics, Vol. 24, No.3, 704-713, Sept., (1994).
15. M.F. Haque and S. Arajs, Brazilian Journal of Physics,Vol. 25, No.4, 257-271, Dec. (1995).
16. R.O. Warrington and R.E. Powe, Int. J. Heat Mass Transfer, 28, 319 (1985).
17. M. Al-Arabi and M. Khamis, Int. J. Heat Mass Transfer 25, 3(1982).
18. S.W. Churchill and H.H.S. Chu, Int. J. Heat Mass Transfer, 8, 1049 (1975).
19. A.J. Chapman, Heat Transfer, 4th ed., New York, MacMilan Publishing Company (1984).